Cell surface receptor kinase FERONIA linked to nutrient sensor TORC1 signaling controls root hair growth at low temperature in *Arabidopsis thaliana*

Javier Martínez Pacheco[1,*], Limei Song[2,*], Victoria Berdion Gabarain[1], Juan Manuel Peralta[1], Tomás Urzúa Lehuedé[3,4], Miguel Angel Ibeas[3,4], Sirui Zhu[2], Yanan Shen[2], Feng Yu[2,†] & José M. Estevez[1,3,4,†]

[1]Fundación Instituto Leloir and IIBBA-CONICET. Av. Patricias Argentinas 435, Buenos Aires C1405BWE, Argentina.

[2]State Key Laboratory of Chemo/Biosensing and Chemometrics, College of Biology, and Hunan Key Laboratory of Plant Functional Genomics and Developmental Regulation, Hunan University, Changsha 410082, P.R. China.

[3]Centro de Biotecnología Vegetal, Facultad de Ciencias de la Vida, Universidad Andres Bello.

[4]ANID - Millennium Science Initiative Program - Millennium Institute for Integrative Biology (iBio) and Millennium Nucleus for the Development of Super Adaptable Plants (MN-SAP), Santiago, Chile.

*Co-first authors.

[†]Correspondence should be addressed. Email: feng_yu@hnu.edu.cn (F.Y) and jestevez@leloir.org.ar (J.M.E).

Abstract

Root hairs (RH) are excellent model systems for studying cell size regulation since they elongate several hundred-fold their original size. Their growth is determined both by intrinsic and environmental signals. Although nutrients availability in the soil are key factors for a sustained plant growth, the molecular mechanisms underlying their sensing and downstream signaling pathways remains unclear. Here, we identified the low temperature (10°C) triggers a strong RH cell elongation response involving the cell surface receptor kinase FERONIA (FER) and the nutrient sensing role of TOR Complex 1(TORC1). We found that FER is required to perceive limited nutrients availability caused by low temperature, to interacts with and activate TORC1-downstream components to trigger RH growth. We also found that nitrate availability could mimic the RH growth response at 10°C via an unknown specific mechanism involving the NRT1.1 transceptor. Our findings reveal a new molecular mechanism by which a central hub composed by FER-TORC1 might be involved in the control of RH cell elongation under low temperature.

Abstract Word counts 164

Text Word counts 3,377

Figures 1-5

Figure S1-S3

Introduction

Root hairs (RHs) are single cells that develop as a cylindrical protrusion from the root epidermis in a developmentally regulated manner. RHs are able to expand in a polar manner several hundred times their original size in a couple of hours to reach water-soluble nutrients in the soil, to promote interactions with the local microbiome, and to support the anchoring of the plant. RH growth is controlled by the coordination of a plethora of environmental and endogenous factors[1]. Recently, an autocrine mechanism of RH growth was described where RALF1-FER complex recruits and phosphorylates the early translation factor eIF4E1 to enhance protein synthesis of specific mRNAs, including the RH growth master regulator: *ROOT HAIR DEFECTIVE SIX-LIKE4 (RSL4)*[2]. It is known that macronutrients availability are key factors that promotes rapid RH growth[1,3,4]. Although nitrate is detrimental to RH growth, their mechanisms of action remain unknown[5–7] . The CHLORINA1/NITRATE TRANSPORTER1.1 (CHL1/NRT1.1) was proposed as a transceptor (transporter and receptor) for nitrates[8–10] as well as for auxin transport[11]. When the position T101 of NRT1.1 is phosphorylated, NRT1.1 becomes a high-affinity NO_3^- (nitrate) transporter, giving this protein a dual-affinity capability[12–15] . Recently, we have shown that at low temperature conditions (at 10 °C), nutrients availability in the media is reduced and triggers an exacerbated RH growth that is suppressed if nutrients are increased[16]. Although great advances were achieved in our understanding on how RH growth occurs at low temperature, it is still unclear how nutrient availability derived from low temperature is perceived in the RH cells and which are the non-transcriptional responses that control RH growth.

TARGET OF RAPAMYCIN (TOR) is an evolutionarily conserved Ser/Thr protein kinase in all eukaryotic organisms that acts as a central growth regulator controlling metabolism and protein synthesis[17–19] .TOR is found in at least two distinct multiprotein complexes called TOR Complex 1 and 2 (TORC1 and TORC2), although only TORC1 was experimentally validated in plants[20,21] . The *Arabidopsis* TORC1 complex is encoded by one *TOR* gene (*At*TOR)[22] ,two *REGULATORY-ASSOCIATED PROTEIN OF TOR (RAPTOR A and B)* genes[23–28], and two *LETHAL WITH SEC THIRTEEN 8 (LST8)* genes[29]. In contrast to the embryo-lethal *tor*-null mutant lines, *raptor1b* and *lst8-1* mutants are viable but show significant growth issues and developmental phenotypes[30]. Some canonical downstream targets of TOR are conserved in plants, such as the S6 kinase (S6K) which stimulates protein translation[25,31–34]. In plants, TORC1 complex plays a key role during many stages of the plant life cycle by controlling both anabolic and catabolic downstream processes. In addition, TORC1 is activated by nutrient availability and inactivated by stresses that alter cellular homeostasis[19,35–39]. The TORC1 complex senses and integrates signals from the environment to coordinate developmental and metabolic processes including hormones (e.g., auxin), several nutrients (e.g., Nitrogen and Sulfur), amino acids and glucose[17,28,40–44]. However, the underlying molecular mechanisms by which TORC1 operates at a single plant cell level has yet to be elucidated. Although

the sensing and uptake of nutrients by RHs is crucial for the plant productivity, the molecular mechanisms underlying these processes remain unknown. Until now, few upstream regulators of TOR have been described in plants. Among them, there is a single subfamily of Rho GTPases (ROPs) involved in the spatial control of cellular processes by signaling to the cytoskeleton and vesicular trafficking. Particularly, ROP2 GTPase activates TOR in response to auxin and nitrogen signals[44–46]. In addition, ROP2 is described as a monomeric GTP-binding protein that participates in many cellular signaling processes, including the polar growth of pollen tubes and root hairs[47–50]. ROPs activation is regulated by ROP guanine nucleotide exchange factors (ROP-GEFs) which interact with several receptor-like kinases (RLKs) including the *Cr*RLK family member: FERONIA (FER)[48]. During the cell elongation of RH, ROP2 is activated by the ROPGEF1-FER interaction. This process is also regulated by ROP-GEF4 and ROP-GEF10[48,51] .Therefore, ROP2 (among other ROPs) may bridge the membrane receptor FER with TORC1 activation, although this was not yet demonstrated.

FERONIA was also linked to carbon/nitrogen balance during the plant growth[52]. Even more, it was shown that the cytoplasmic kinase domain of FER and its partner RIPK (RPM1-induced protein kinase) interact with TOR and RAPTOR-A forming a complex to positively modulate TOR pathway under nutrient starvation. Currently, it is clear that plant growth can be affected via FER-TOR axis since they act early by linking amino acid and/or nutrients signaling with global protein synthesis[52]. Existing evidences suggest that nutrient mediated sensing at the cell surface level triggers a response thought the TOR signaling pathway. However, it is still unknown which are the environmental signals activated in RH by the FER-TORC1 pathway. Taking into account that previously we described that a low temperature stress is able to trigger an exacerbated RH growth[16,53], this stress condition was used as a proxy to investigate which are the environmental signals that activate RH cell elongation. Our research reveals a novel mechanism in which FER and TORC1 are necessary to regulate RH growth in *Arabidopsis* in the context of the nutrient availability (nitrate) as cause of low temperature stress.

Results

FER is required to trigger a strong RH growth response at low temperature. Here, we asked which might be the cell surface protein involved in perceiving and/or transducing the low temperature stimulus. Since FER was shown as an important hub between the cell surface signaling with downstream processes during RH growth[2,48] ,we tested if the *fer-4* null mutant and *fer-5* (a truncated version with shortened kinase domain (KD)) are able to respond to low temperature stimulus. Both *fer* mutants failed to trigger RH growth regardless the temperature (**Figure 1A**). On the contrary, the related CrRLK1L ERULUS (ERU), previously linked to RH growth and cell wall integrity processes with a severe short cell elongated RH phenotype at 22°C[54,55], was able to react

to low temperature and triggered a RH growth response although to a lower extent than Wt Col-0. This indicates that FER, but not ERU, might be involved specifically in this growth response despite being phylogenetically related[55] .Then, a fluorescent translational reporter line of FER (FER*p*:FER-GFP), was used to study *FER* expression in RHs in two growth stages, an initial and a later stage. FER is clearly activated under low temperature stimulus at the initiation stage of RH growth and to a lower extent at a later stage (**Figure 1B**). Finally, phosphorylated and non-phosphorylated levels of FER (FER-p/FER) were quantified at both temperatures. Under low temperature, almost half of the FER protein levels was present as a non-phosphorylated form and after 3 days of growth, almost all FER protein was present as a phosphorylated version (**Figure 1C**). This indicates that low temperature not only increases FER protein levels in growing RHs at the plasma membrane but also promotes a complete phosphorylation of FER protein, possibly enhancing the interaction with putative partners and triggering the activation of downstream signaling components of RH polar growth.

TORC1 pathway is involved in low temperature induced RH growth. Recently, it was shown that FER-RIPK interacts with TOR-RAPTOR and phosphorylates it leading to the TOR pathway activation in the context of nutrient perception and global metabolism regulation. We then asked if TOR might be also involved in the RH growth process under low temperature. In the first place, a β-estradiol (es)-induced TOR knockdown (*tor-es,* es-induced RNAi silencing of TOR) line[56] showed short RHs as previously has been reported[33] and notably, a lack of response to low temperature stimulus (**Figure 2A**). Secondly, in a similar manner, inhibition of TOR kinase activity with AZD-8055[57], a novel ATP-competitive inhibitor of mTOR kinase activity, abolished the RH growth at both 22°C and low temperature (**Figure 2B**). On the other hand, overexpression of TOR enhanced RH growth at both temperatures assayed (**Figure 2C**). These results lead us to suggest that the TOR pathway is involved in the RH low temperature growth response and might operates downstream of FER. At the transcriptional level, TOR expression levels are upregulated in roots up to three-folds at 10 °C vs 22 °C (**Figure S1**). To deepen in this study, we tested if the growth response at low temperature in RHs is also affected in mutants of the TORC1 pathway and some downstream components. All the mutants *(raptor1b, rps6b,* and *lst8-1)* were all unable to respond to the low temperature treatment but their RHs phenotypes showed a broad spectrum of responses in terms of cell length with respect to the Wt Col-0 (**Figure 2C**). For instance, *raptor1b* behaved similarly to *tor-es* mutant, while *rps6b* had an intermediate phenotype and *lst8* was comparable to Wt Col-0 (at 22°C) (**Figure 2C**). In addition, the overexpression of TOR and the S6 kinase 1 (S6K1), as a direct downstream target of TOR, showed enhanced RH growth at 22 °C. Since previous reports showed that phosphorylation of the ribosomal S6K1 can be used to monitor TOR protein kinase activity in plants[33,56] ,we measure the ratios of S6K-p/S6K. Lower levels of S6K-p/S6K were detected for those lines with strong short RH phenotype (mutants in components of the TORC1 complex and in FER protein) while those with longer RHs (overexpression of S6K1 and TOR) showed higher ratios

(**Figure 2D, 3D**). These results clearly indicate that TORC1 and some downstream components (e.g. S6K) promote RH growth under low temperature.

FER regulates TOR polar localization in RH and activation of TORC1 pathway at low temperature. Since TORC1 activation under a plethora of stimuli usually triggers the phosphorylation of the downstream factor S6K (S6K-p), we asked if low temperature responses regulated by FER might control this output. With this in mind, we investigated the molecular mechanisms by which TORC1-S6K are induced at 10 °C and we tested whether this might be mediated by FER. Since *fer-4* and *tor-es* showed a similar RH phenotypes at low temperature (**Figure 2A-B**), possibly indicating that they may act in the same pathway, we first tested if FER and TOR interaction is enhanced under 10°C vs 22°C. By performing a co-immunoprecipitation (Co-IP) analysis, we found that FER-TOR protein-protein interaction is enhanced under low temperature (**Figure 3A**). This confirms a direct interaction between FER and TOR kinase in low temperature RH mediated growth. Then, by evaluating the immunolocalization of TOR in the growing RHs, we found that FER is required for the apical accumulation of TOR since TOR lost the polar pattern in *fer-4* root hairs. In addition, the level of RH tip-localized TOR detected was similar at both, low temperature and control conditions (22°C) (**Figure 3B-C**). This indicates that in root hairs, TOR is able to localize into the tip and this is dependent on FER. Then, it was tested if FER is involved in the S6K activation by TOR by measuring the ratio of S6K-p/S6K proteins under both growth conditions in Wt Col-0, *fer-4*, *fer-5*, and FER^{K565R}, which has been shown to abolish FER autophosphorylation and transphosphorylation in an *in vitro* kinase activity assay[58,59] ,although some activity might remain[60]. Interestingly, low temperature enhanced S6K-p levels after 3 days of growth in Wt Col-0 at low temperature but this was partially suppressed in all *fer* mutants tested (**Figure 3D**). This suggests that FER controls the level of TORC1 activation under low temperature in RH. Collectively, these results indicate that TOR localization in the RH tip and TORC1 activation is dependent on FER and enhanced at low temperature.

Nitrate perception and transport mediated by NRT1.1 controls RH growth at low temperature. Previous studies have been shown that nitrogen and specifically nitrates are important nutrient for TOR signaling[44,61] . Since low temperature growth conditions reduce the availability of nutrients in the media and trigger a strong response in RH growth[16,53] , we decided to test if nitrate signaling pathway might be involved. We found that high levels of nitrate (18.8 mM) were able to repress low temperature mediated RH growth while low levels of nitrate (0.5 mM) did not affect growth under this temperature (**Figure 4A**). This clearly indicated that nitrate is one of the major growth signals that activate RH cell elongation at low temperature where there is a low nutrient mobility environment. Then, we tested if the dual affinity nitrate transporter and sensor NRT1.1 is involved in this low temperature RH growth response. The NRT1.1 null mutants *chl1-5*, *chl1.9* (NRT1.1 harbors a substitution P492L that suppresses its root nitrate uptake activity[8] ,as well as the catalytically inactive $CHL1^{T101D}$ version showed a strong RH growth response despite the

temperature conditions (**Figure 4B**), similarly to *S6K1-OE* and *TOR-OE* lines (**Figure 2C**), but to a lower extent in terms of RH cell elongation. As expected, similar levels of S6K-p/S6K were detected in the *chl1-9* line at both temperatures (**Figure 4C**). When these NRT1.1 mutants were grown under high (18.8 mM) or low (0.5mM) nitrate concentrations at both temperatures (at 22°C and at 10°C), a similar RH phenotype was detected between both nitrate conditions either at 22 °C or 10 °C (**Figure 4D**). On the contrary, as expected Wt Col-0 RH were sensitive to both, low temperature and nitrate levels. Overall, this suggested a key role of NRT1.1 in the perception of changes in nitrate levels and in the regulation of the downstream TORC1-S6K activation. At this point, we hypothesized that FER might be a good candidate to controls NRT1.1 activity under low temperature (and low nitrate), but this remains to be tested.

ROP2 is required for low temperature RH growth. Previous studies have shown a key role of ROP2 in the regulation of RH polarity and elongation[49,62,63], as an important molecular link between FER and downstream components involved in RH growth[48]. In addition, ROP2 promotes the activation of TOR and its relocation to the cell periphery and induces the downstream translation pathway[45]. More importantly, ROP2 was shown to integrate diverse nitrogen and hormone signals for TOR activation[44]. In the first place, *rop2* abolishes the differential growth responses at 10°C and produces a very short RH phenotype (**Figure 5A**). While high levels of TOR are able to enhance RH growth regardless of the temperature treatments (**Figure 2C**), the constitutively active ROP2 version (CA-ROP2) is able to repress TOR activation (**Figure 5A**). As expected, 35S-TOR-GFP (TOR OE) with constitutive long RHs at both temperatures showed much higher levels of S6K-p/S6K than Wt Col-0 while the presence of CA-ROP2 (in TOR OE/CA-ROP2) was able to reduce the levels of S6K-p/S6K linked to a diminished RH growth (**Figure 5B**). Then, we asked if TOR partition between plasma membrane/cell surface-cytoplasmic localization might be changed by the effect of low temperature (equal to reduced nutrient environment) and if this is changed by the presence of CA-ROP2 (**Figure 5C**). Low temperature triggers a higher cell surface TOR localization while the presence of CA-ROP2 abolishes this effect. Taken together, we observed a direct effect of CA-ROP2 version in the TOR localization at the RH tip, RH growth responses and TORC1 activation. Then, we tested if a treatment with exogenous auxin (100 nM IAA) that is able to trigger a strong RH growth response and ROP2 activation, might be able to bypass silenced TOR growth inhibition effect in RH at both, room and low temperatures (**Figure S2**). In this case, auxin treatment was able to partially revert RH growth inhibition under TOR silenced line. Because of ROP2 activity and other possible unknown effectors, auxin is able to partially rescue RH growth when TOR is inhibited, highlighting that other pathway might be still being active downstream auxin independently of TORC1 to trigger RH cell elongation.

Discussion

Growth and development of plants and animals are based on nutrient and hormonal signaling that constitute as the main regulatory networks in eukaryotes. Unraveling the functions of the regulatory hubs and their detailed molecular mechanisms are critical for understanding the deepened modes of regulation in these signaling pathways. Our study uncovers a new molecular mechanism by which plants use FER-ROP2-TORC1 signaling pathway to control cell elongation in RH under nutrient starvation induced by low temperature stress. Here we showed that the cell surface FER receptor is able to regulate TOR apical localization and further downstream activation, both controlling S6K phosphorylation linked to RH growth. Based on the results obtained, here we propose a model in which the FER-ROP2-TORC1 axis might be able to regulate the RH growth under low temperature with remarked attention to variable nitrate conditions (**Figure S3**). It is based on the mutants tested in this signaling pathway, FER-TOR enhanced interactions, TOR polar localization in RHs and S6K-p/S6K as a TORC1 activation response. Changes in nitrate concentrations in the media mimicked this response at low temperature and mutants on the NRT1.1 transceptor are insensitive at RH growth level regardless the temperature or nitrate levels. We hypothesize that low nitrate in the media might rapidly induce the levels of mature-active RALF1 (and possibly other RALF peptides), which might then activate FER-ROP2-TORC1 pathway and the downstream fast cell elongation effect to search for further nutrients sources. This autocrine mechanism dependent on RALF1-FER growth activation has been recently demonstrated for RH[2,64] ,but not in a context that involves low temperature/low nitrate and TORC1 pathway. Finally, several questions in our proposed model (**Figure S3**) remain to be answered in future studies. How does low nitrate concentration (low temperature) triggers FER-TORC1 activation? Does RALF1 and other RALFs respond to low nitrate to activate FER? Does FER activate NRT1.1 directly? Recently, it was shown that FER-regulated ROP2 triggers a new mechanism for the negative regulation of rhizosphere microorganisms such as *Pseudomonas*[65] .Although not tested here, FER-ROP2-TORC1 signaling coupled to enhanced RH growth under low temperature (low-nutrients) might be linked in root growth in specific soil conditions to select favorable microbiota in the soil. This pathway may integrate complex signals from soil nutrients and microbiota in the rhizosphere to plant root cell growth mechanism.

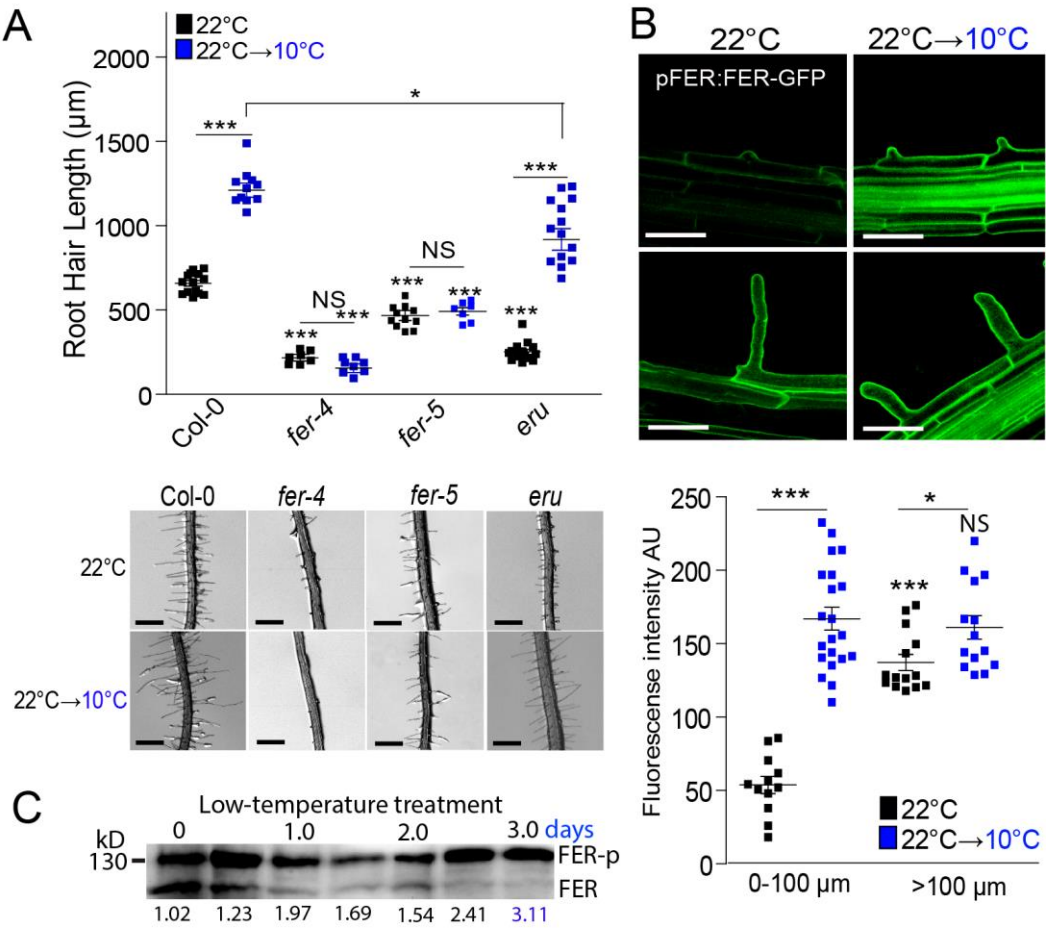

Figure 1. High levels of FER in its phosphorylated form is required to trigger the low temperature RH growth.

(A) Scatter-plot of RH length of Col-0, of *fer-4*, *fer-5*, and *eru* mutants grown at 22°C or at 10°C. RH growth is enhanced at low temperature in Wt Col-0 and *eru* mutant but not in the *fer-4* and *fer-5* mutants. Each point is the mean of the length of the 10 longest RHs identified in a single root. Data are the mean ± SD (N=10-20 roots), two-way ANOVA followed by a Tukey–Kramer test; (*) p <0.05, (***) p <0.001, NS=non-significant. Results are representative of three independent experiments. Asterisks indicate significant differences between Col-0 and the corresponding genotype at the same temperature. Representative images of each genotype are shown below. Scale bars= 500 µm. (B) Confocal images of the reporter line of FER in two growth stages of RH cells, short RHs (on top) and long RHs (on the bottom) at 22°C *vs* low temperature (10°C). Below, quantification of the GFP fluorescence intensity in RH tip. Fluorescence AU data are the mean ± SD (N=11-20 root hairs), two-way ANOVA followed by a Tukey–Kramer test; (*) p < 0.05, (***) p < 0.001. Results are representative of two independent experiments. Asterisks on the graph indicate significant differences. Scale bars: 100 µm.

278 (C) Phosphorylation levels on FER (FER-p in *p*FER:FER-GFP) increases after 3 days at low
279 temperature in roots. Phosphorylated levels of FER were analyzed by ImageJ.

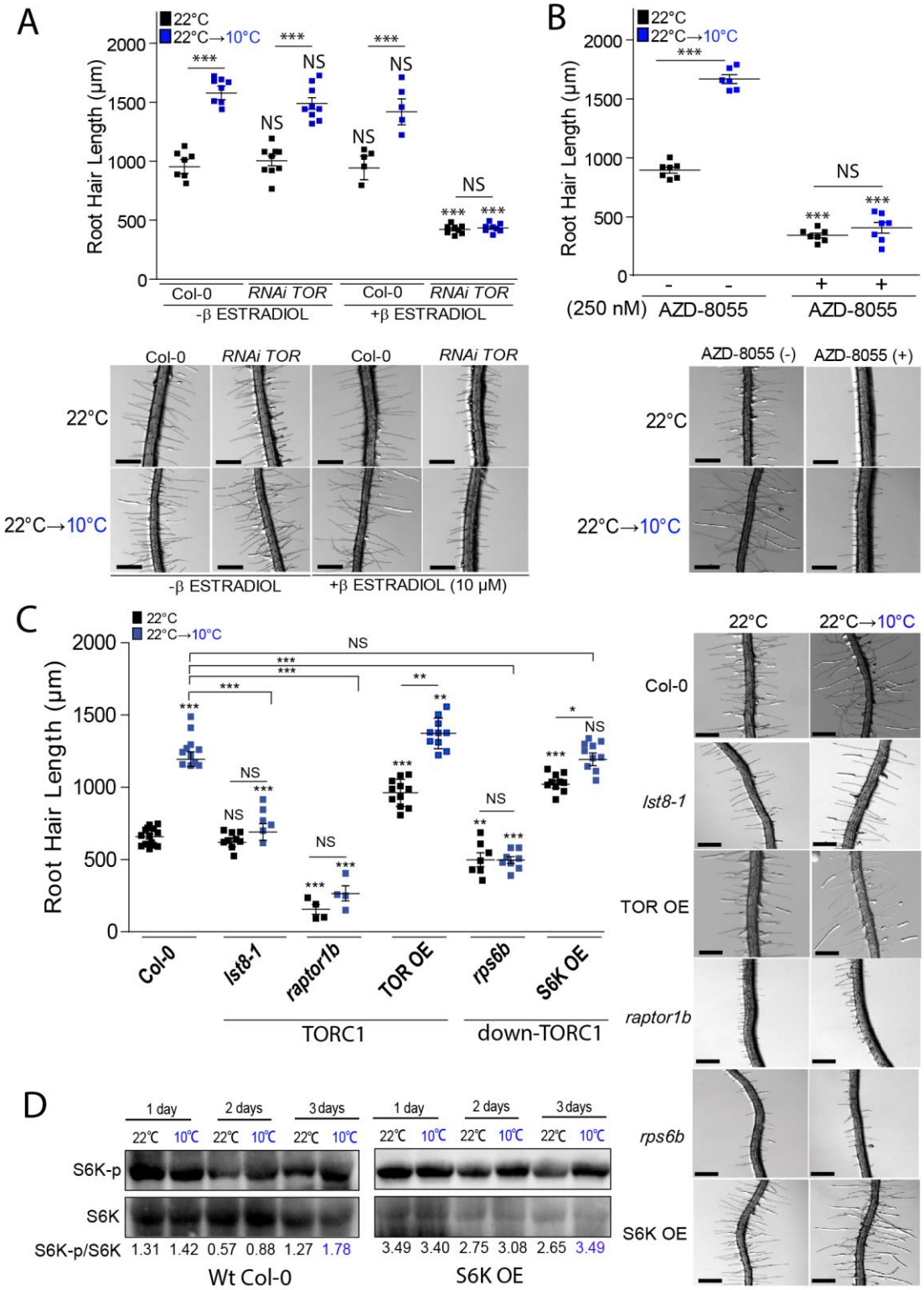

Figure 2. TORC1 signaling pathway is required for low temperature triggered RH growth.

(A) Scatter-plot of RH length of Col-0 and *tor-es* line grown at 22°C or at 10°C. Differential growth of RH at low temperature is suppressed in the estradiol inducible *RNAi TOR* line. Each point is the mean of the length of the 10 longest RHs identified in a single root. Data are the mean ± SD (N=7-10 roots), two-way ANOVA followed by a Tukey–Kramer test; (***) p <0.001, NS=non-significant. Results are representative of three independent experiments. Asterisks indicate significant differences. Representative images of each line are shown below. Scale bars= 500 µm.

(B) Differential growth of RH at low temperature is abolished in the Col-0 treated with 250nM of TOR inhibitor, AZD-8055. Each point is the mean of the length of the 10 longest RHs identified in a single root. Data are the mean ± SD (N=7 roots), two-way ANOVA followed by a Tukey–Kramer test; (***) p <0.001, NS=non-significant. Results are representative of three independent experiments. Asterisks indicate significant differences. Representative images of each line are shown below. Scale bars= 500 µm.

(C) RH cell elongation of TORC1 and downstream TORC1 signaling pathway mutants under low temperature. Each point is the mean of the length of the 10 longest RHs identified in a single root. Data are the mean ± SD (N=7-12 roots), two-way ANOVA followed by a Tukey–Kramer test; (*) p <0.05, (**) p <0.01, (***) p <0.001, NS=non-significant. Results are representative of three independent experiments. Asterisks indicate significant differences. Representative images of each line are shown on the right. Scale bars= 500 µm.

(D) Analysis of the phosphorylation state of S6K (S6K-p/S6K ratio) in Col-0 and *S6K-OE* line. A representative immunoblot is shown of a three biological replicates. S6K-p/S6K ratio was analyzed by ImageJ.

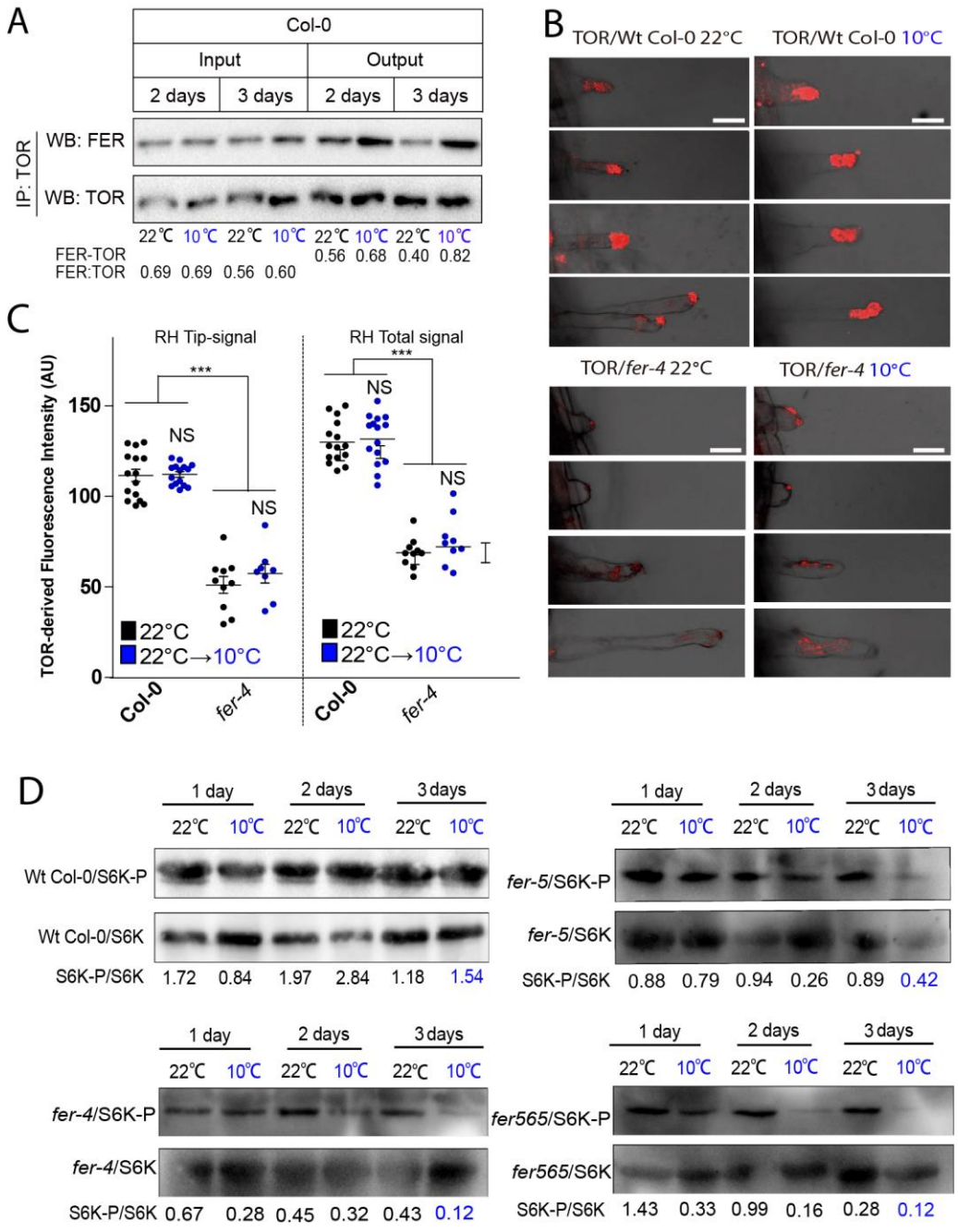

Figure 3. **FER controls apical TOR localization and subsequent activation thus increasing phosphorylation of S6K under low temperature.** (A) Enhanced FER-TOR interaction at low temperature in roots by Immunoprecipitation (IP). A representative experiment of three replicates is shown.

(B) On the top, TOR immunolocalization in RHs is FER-dependent. Scale bar=20 µm

(C) Apical and total TOR signal quantification in RHs showed in (B). A ROI at the RH tip of the fluorescent signal or all the RH TOR-derived fluorescent signal was measured. Fluorescence AU

data are the mean ± SD (N=10-15 root hairs), two-way ANOVA followed by a Tukey–Kramer test; (***) $p < 0.001$, NS= non significant. Results are representative of two independent experiments. Asterisks on the graph indicate significant differences.

(D) Analysis of the phosphorylation state of S6K in Wt Col-o, *fer-4, fer-5*, and *FER*^{K565R} mutants Arabidopsis roots. Phosphorylation of S6K (S6K-p) is enhanced at low temperature and requires FER active kinase. A representative immunoblot is shown of a three biological replicates. S6K-p/S6K ratio was analyzed by ImageJ.

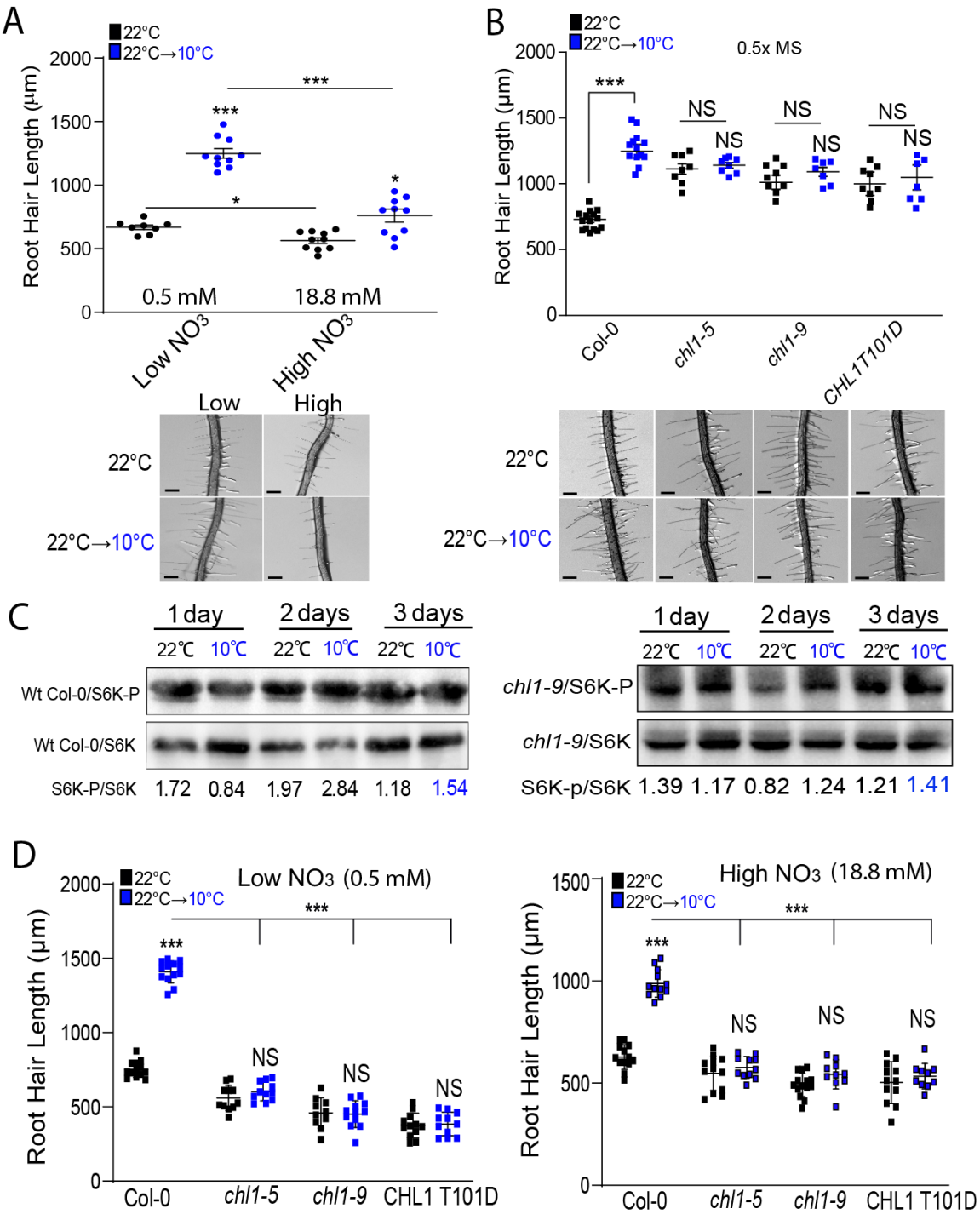

Figure 4. Nitrate acts as a RH growth signal perceived by NRT1.1 and triggered by TORC1 pathway at low temperature growth.

(A) High nitrate (18.8 mM) suppresses low temperature enhanced RH growth in Wt Col-0 plants. . Each point is the mean of the length of the 10 longest RHs identified in a single root. Data are the mean ± SD (N=10 roots), two-way ANOVA followed by a Tukey–Kramer test; (*) p <0.05, (***) p

<0.001. Results are representative of three independent experiments. Asterisks indicate significant differences. Representative images of each line are shown below. Scale bars= 500 µm.

(B) Low temperature RH growth is regulated by the nitrate sensor NRT1.1 (CHL1). Scatter-plot of RH length of Col-0 in low or high nitrate conditions(right); RH length of Col-0 and NRT1.1 mutants, (left) grown at 22°C or 10°C. Each point is the mean of the length of the 10 longest RHs identified in a single root (N=15-20). Each point is the mean of the length of the 10 longest RHs identified in a single root. Data are the mean ± SD (N= 10-15 roots), two-way ANOVA followed by a Tukey–Kramer test; (***) p <0.001, NS= non-significant. Results are representative of three independent experiments. Asterisks indicate significant differences. Representative images of each line are shown below. Scale bars= 500 µm.

(C) Analysis of the phosphorylation state of S6K in Wt Col-0 and *chl1-9* mutant roots. A representative immunoblot is shown of a three biological replicates. S6K-p/S6K ratio was analyzed by ImageJ.

(D) RH growth responses under high and low nitrate (18.8 mM and 0.5mM, respectively) in Wt Col-0, *chl1-5*, *chl1-9* mutants, and $CHL1^{T101D}$ grown at 22°C or 10°C. Each point is the mean of the length of the 10 longest RHs identified in a single root. Data are the mean ± SD (N= 10-15 roots), two-way ANOVA followed by a Tukey–Kramer test; (***) p <0.001, NS= non-significant. Results are representative of three independent experiments. Asterisks indicate significant differences.

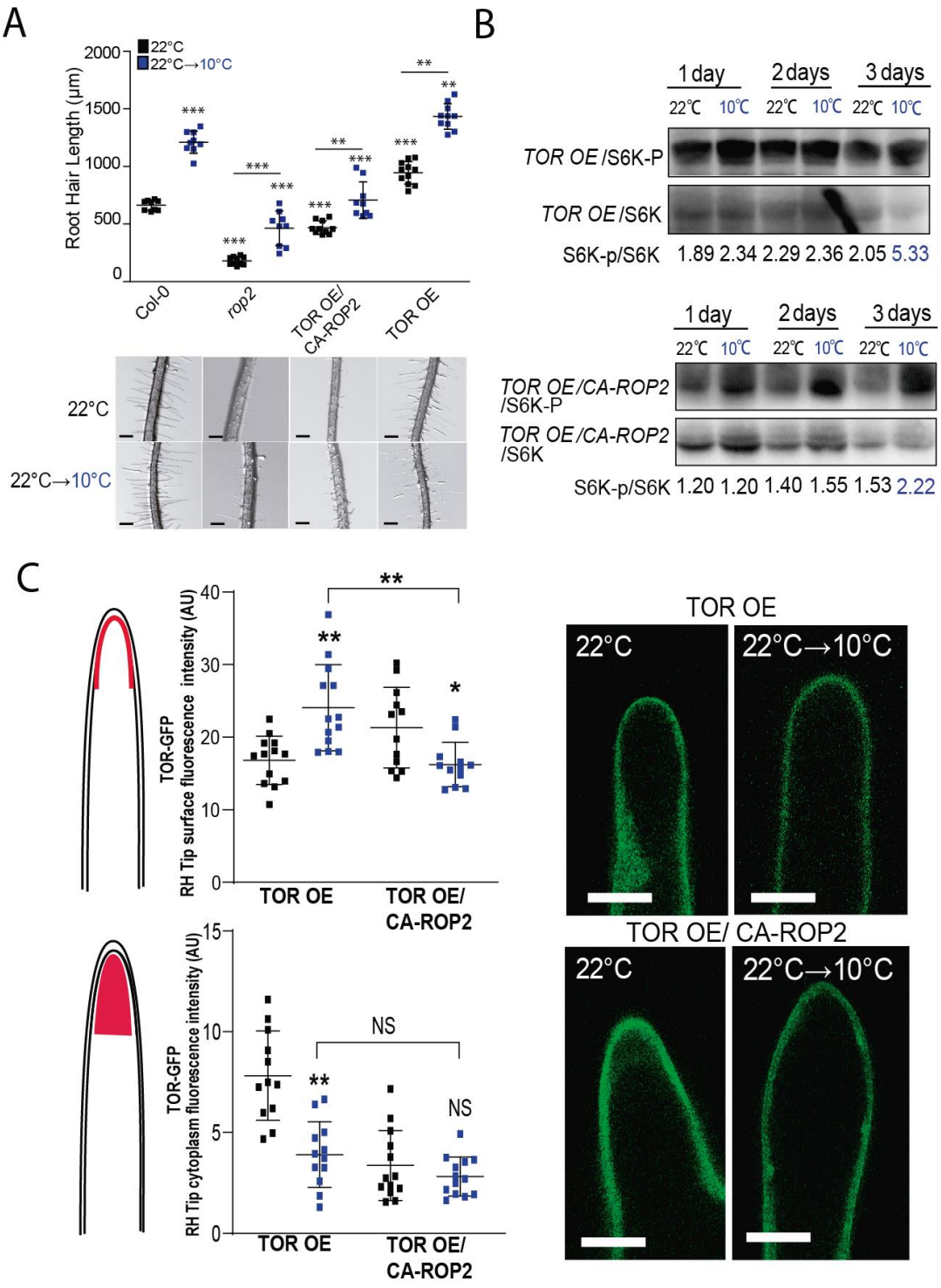

Figure 5. ROP2 is required to triggers RH growth at low temperature. (A) ROP2 is required for RH at low temperature meanwhile *rop2* and CA-ROP2/35S-TOR block RH growth. Each point is the mean of the length of the 10 longest RHs identified in a single root. Data are the mean ± SD (N= 10-15 roots), two-way ANOVA followed by a Tukey–Kramer test; (**) p <0.01, (***) p <0.001. Results

are representative of three independent experiments. Asterisks indicate significant differences. Representative images of each line are shown below. Scale bars= 500 µm.

(B) Analysis of the phosphorylation state of S6K in *TOR-OE* and *TOR-OE / ROP2-CA Arabidopsis* roots. Phosphorylation of S6K (S6K-p) is enhanced in *TOR-OE* and suppressed in *TOR-OE*/ROP2-CA. A representative immunoblot is shown of a three biological replicates. S6K-p/S6K ratio was analyzed by ImageJ.

(C) Quantification of TOR-GFP localization in the cell surface versus cytoplasmic localization in the RH tip in Wt Col-0 and in CA-ROP2 background. Fluorescence AU data are the mean ± SD (N=12-15 root hairs), two-way ANOVA followed by a Tukey–Kramer test; (*) $p < 0.05$, (**) $p < 0.01$, NS= non-significant. Results are representative of two independent experiments. Asterisks on the graph indicate significant differences. Representative images of each line are shown on the right. Scale bars= 1 µm.

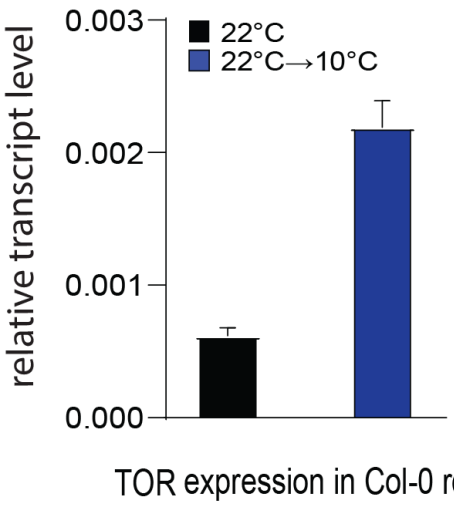

Figure S1. Quantitative PCR of *TOR* expression levels in Col-0 roots grown at 22°C and 10°C. *ACT2* expression was used for normalization of gene expression. Three biological replicates and three technical replicates per experiment were performed**.**

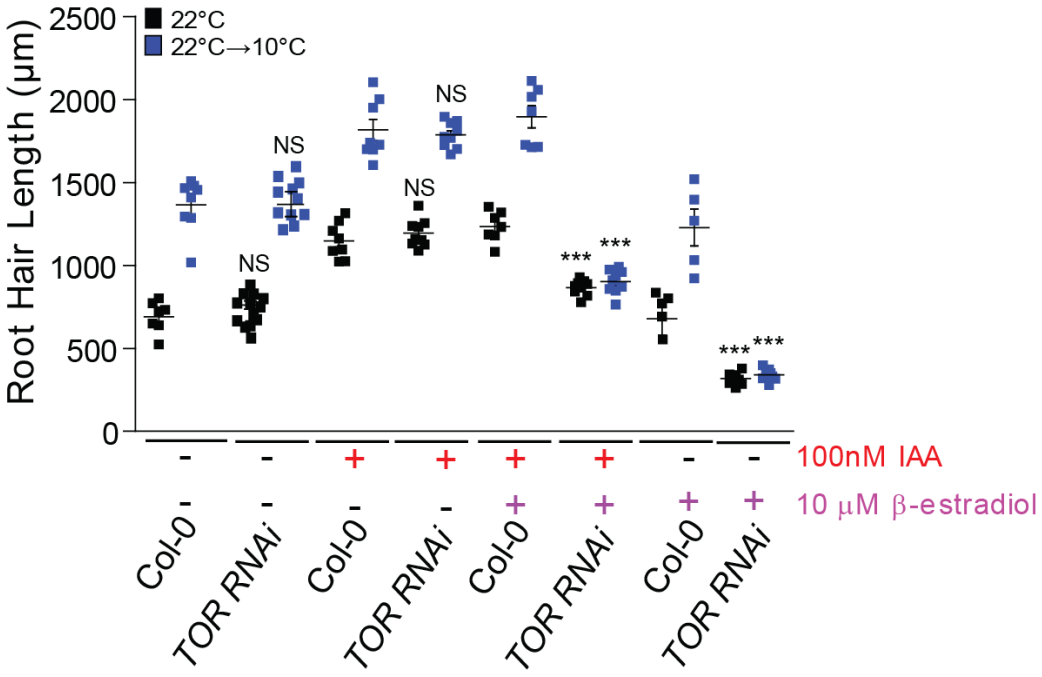

Figure S2. TOR-pathway on RH growth is partially dependent on auxin.

RH length of non-treated and treated Col-0 and TOR-RNA*i* line (*tor-es*) with 100nM IAA at 22°C *vs* 10°C. Each point is the mean of the length of the 10 longest RHs identified in a single root. Data are the mean ± SD (N= 10-15 roots), two-way ANOVA followed by a Tukey–Kramer test; (***) p <0.001, NS=non-significant. Results are representative of three independent experiments. Asterisks indicate significant differences.

Low temperature perception by FER-TORC1 triggers root hair growth

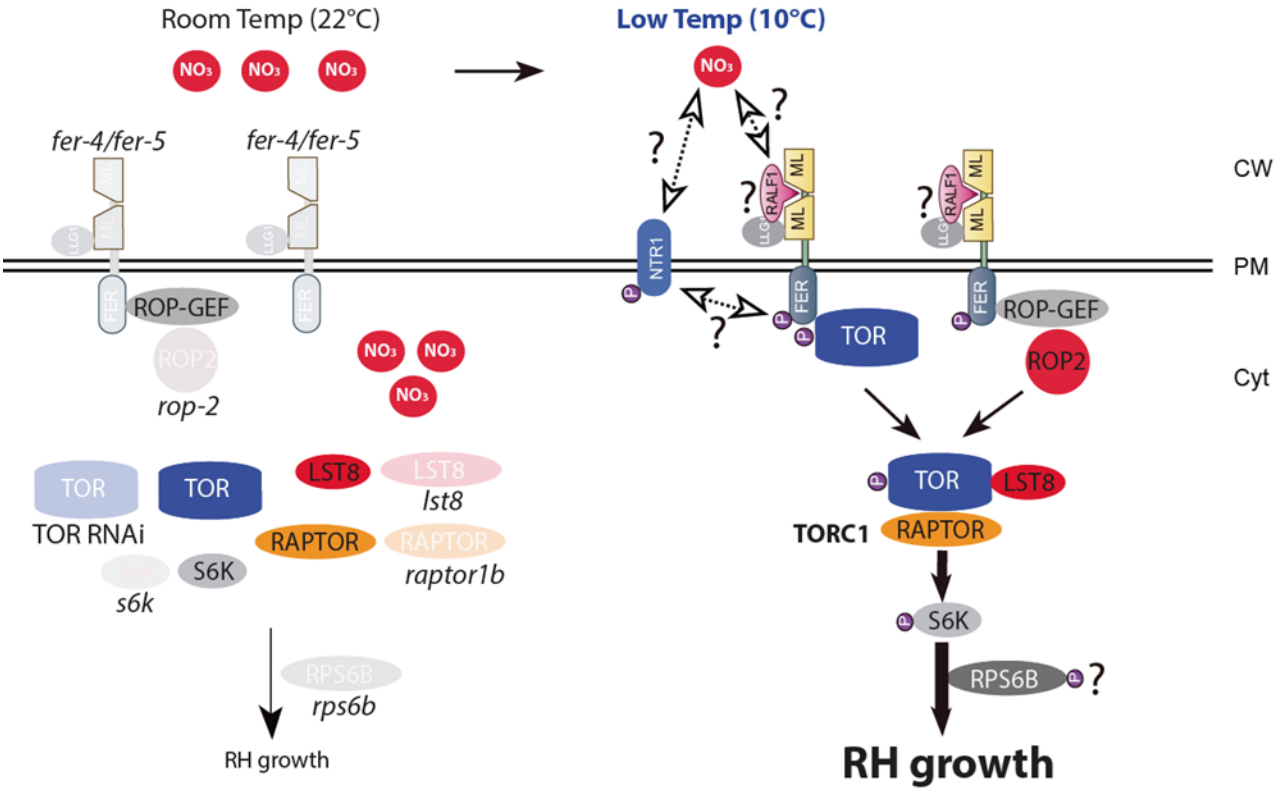

Figure S3. **Proposed model of FER-ROP2-TORC1 pathway at low temperature-nitrate that triggers cell elongation in RHs**. On the left, several mutants characterized in this work. On the right, the model based on the current evidence shown in this work and together with previous works. Low temperature triggers a low nitrate environment that leads to FER activation, enhanced FER-TOR interaction and TORC1 activation. This promotes cell elongation of RHs. This response also requires ROP2 that might bridge FER with TORC1. Several questions (?) remain to be answered in future studies such as how low nitrate (low temperature) triggers FER-TORC1 activation? Does FER activate NRT1.1 directly? Do RALF1 and other RALFs respond to low nitrate to activate FER?.

Experimental Procedures

Root hair phenotype. Seeds were surface sterilized and stratified in darkness for 3 days at 4°C. Then grown on ½ strength MS agar plates supplemented with MES (Duchefa, Netherlands), in a plant growth chamber at 22°C in continuous light (120 µmol.sec-1.m-2) for 5 days at 22°C plus 3 days at 10°C (moderate-low temperature treatment) or for 8 days at 22°C as control. For quantitative analyses of RH phenotypes, 10 fully elongated RH from the maturation zone were measured per root under the same conditions from treatment and control. Measurements were made after 8 days. Images were captured using an Olympus SZX7 Zoom Stereo Microscope (Olympus, Japan) equipped with a Q-Colors digital camera and Q Capture Pro 7 software (Olympus, Japan). Results were expressed as the mean ± SD using the GraphPad Prism 8.0.1 (USA) statistical analysis software. Results are representative of three independent experiments, each involving 7–20 roots.

Plant Material and Growth Conditions. Plants were grown on agar plates in a plant chamber at 22 °C for 7 days at 24 hs light (120 µmol.seg-1.m-2). *A. thaliana* Col-0 ecotype was used as a wild-type plant. A Murashige & Skoog-based media without N, P nor K (M407, PhytoTechnology Laboratories, https://phytotechlab.com/) was used as the growth base medium under sterile conditions. To test the low and high nitrate response, 0.5X M407 media was supplemented with 0.8% plant agar (Duchefa, Netherlands); 1.17mM MES,0.625 mM KH_2PO_4 monobasic and 0.5mM or 18.8 mM KNO_3, respectively. Plants were treated for the indicated period in accordance with prior conditions. *chl1-5*, *chl1-9 and T101D* mutants were kindly donated by Dr Yi-Fang Tsay. *tor-es* was kindly donated by Dr Ezequiel Petrillo, *lst8-1*, *rps6b*, *raptor1b* and overexpressing line S6K1 kindly donated by Dr Elina Welchen and *35S::GFP-TOR* and *35S::GFP-TOR/CA-ROP2* kindly donated by Dr. Lyubov Ryabova.

Pharmacological Treatments. Plants were grown on solid 0.5x MS medium plates at 22°C for 5 days at 24 hs light (110 µmol.seg-1.m-2). Then transferred to plates containing solid 0.5x MS, according with the specific treatment, supplemented with 100nM IAA (auxin treatment), 250nM AZD-8055 (TOR inhibition) or 10 µM β-estradiol (TOR RNA*i* estradiol inducible line). Treatments were incubated at 22 °C for 3 days at 24 hs light (110 $\mu mol.seg^{-1}.m^{-2}$) and then at 10 °C for 3 days at 24 hs light (110 $\mu mol.seg^{-1}.m^{-2}$).

Confocal Microscopy. Confocal laser scanning microscopy for the lines *pFER::FER-GFP, 35S::GFP-TOR and 35S::GFP-TOR/CA-ROP2*, was performed using a Zeiss LSM 710 NLO microscope (Zeiss, Germany) (Excitation: 488 nm argon laser; Emission: 490-525 nm, EC Plan Neofluar 40X/1.3 Oil or a Zeiss Plan-Apochromat 63X/1.4 Oil objectives). GFP signal at the cell surface and cytoplasm of the RH tip were quantified using ROIs with the ImageJ software. Fluorescence AU were expressed as

the mean ± SD using the GraphPad Prism 8.0.1 (USA) statistical analysis software. Results are representative of two independent experiments, each involving 10–15 roots and approximately, between 10 to 20 hairs per root were observed.

Co-IP assay. For Co-IP assays using A/G agarose and an anti-TOR antibody[33], 30 µL of A/G beads (Thermo Fisher Scientific Inc., 20421) was resuspended and washed three times using NEB buffer (20 mM HEPES [pH 7.5], 40 mM KCl, 5 mM $MgCl_2$) before adding 8 µL of anti-TOR antibody or preimmune serum as a negative control [33] in a total volume of 500 µL of NEB buffer, followed by incubation for 4 h at 4 ˚C. Col-0 seedlings were first grown at 22 ˚C for 5 days then transferred to 22 ˚C or 10 ˚C for 2 days or 3 days. For protein extraction from plants, the collected materials were ground to a fine powder in liquid nitrogen and solubilized with NEB-T buffer (20 mM HEPES [pH 7.5], 40 mM KCl, 5 mM $MgCl_2$, 0.5% Triton X-100) containing 1 × protease inhibitor cocktail (Thermo Fisher Scientific Inc., 78430) and 1 × phosphatase inhibitor (Thermo Fisher Scientific Inc., 78420) and incubated for 1 h on the ice. The extracts were centrifuged at 16,000 g at 4 ˚C for 15 min, and the resultant supernatant was incubated with prepared antibody-beads from the above step. After overnight incubation at 4 ˚C with rotation, the agarose beads were washed five times with the NEB buffer and eluted with elution buffer (0.2 M glycine, 0.5% Triton X-100, pH 7.5). Anti-FER and anti-TOR antibodies[33] were used for immunoblotting to detect the immunoprecipitates.

TOR immunolocalization. Col-0 and *fer-4* seedlings were first grown at 22 ˚C for 4 days before transferred to 22 ˚C or 10 ˚C for 2 days and treatment with or without 1 µM RALF1 for 30min. Then seedlings were collected and incubated for 10 min under vacuum (0.05 MPa) in phosphate-buffered saline (PBS) containing 4% paraformaldehyde and 0.1% Triton X-100. Seedlings were washed gently three times (10 min for each wash) in PBS and then the cell wall was digested in 2% Driselase (Sigma, D8037) in PBS for 18 min at 37 ˚C and washed five times with PBS. The permeability of the seedlings was increased by incubating them in 3% IGEPAL CA-630 (Sigma, 18896) and 10% DMSO in PBS for 18 min, followed by washed three times with PBS. Seedlings were incubated in 2% bovine serum albumin (BSA) (Ameresco, 0332) in PBS for 1.5 h and then incubated with primary TOR antibody[33] (antibody diluted 1:600 in 2% BSA) for overnight at 4 ˚C. The seedlings were washed with PBS for five times. Fluorophore-labeled secondary antibody (goat–mouse secondary antibody, diluted 1:600 in 2% BSA) was incubated with the samples at 37 ˚C for 5 h in the dark. Seedlings were washed five times with PBS before observation. Fluorescent signal detection and documentation were performed using a Nikon confocal laser scanning microscope with a 560-nm band-pass filter for IF555 detection.

S6K-P/S6K immunoblotting detection. For immunological detection of S6K-P and S6K1/2, total soluble proteins were extracted from 50 mg of plant materials grown as indicated previously with 100 µL 2 × Laemmli buffer supplemented with 1% Phosphatase Inhibitor Cocktail 2 (Thermo Fisher

Scientific Inc., 78430). Proteins were denatured for 10 min at 95 ˚C and separated on 10% or 8% SDS-PAGE. Rabbit *At*TOR polyclonal antibodies (Abiocode, R2854-2), rabbit polyclonal S6K1/2 antibodies (Agrisera, AS121855), and S6K1-p (phospho T449) antibody (Abcam, ab207399) were used for immunoblotting.

Quantitative PCR (qPCR). Total root RNA was extracted from plantlets grown *in vitro* at 22 ˚C and 10 ˚C using the RNeasy®Plant Mini Kit (QIAGEN, Germany). One microgram of total RNA was reverse transcribed using an oligo$(dT)_{20}$ primer and the Super Script™ IV RT (Invitrogen,USA) according to the manufacturer's instructions. cDNA was diluted 20-fold before PCR. *q*PCR was performed on a LightCycler®480 Instrument II (Roche, USA) using 2 µL of 5X HOT FIREPol®EvaGreen® qPCR Mix Plus(no ROX) (Solis BioDyne, Estonia), 2 µL of cDNA, and 0.25 µM of each primer in a total volume of 10 µL per reaction. ACT2 (AT3G18780) gene was used as reference for normalization of gene expression levels (ACT2 primers, F: GGTAACATTGTGCTCAGTGGTGG R: CTCGGCCTTGGAGATCCACATC; TOR primers, F: GAAGATGAAGATCCCGCTGA R: GCATCTCCAAGCATATTTACAGC[45]). The cycling conditions were: 95 °C for 12 min., 35 cycles of 95 °C for 15 sec., 60 °C for 1 min. and finally a melting curve from 60 °C to 95 °C (0.05°/sec). Data were analyzed using the $\Delta\Delta C_t$[66] method and LightCycler®480 Software, version 1.5 (Roche). Two independent experiments with three biological and three technical replicates per experiment, were performed.

Acknowledgements

We would like to thank Elina Welchen, Ezequiel Petrillo, Lyubov A. Ryabova, Yi-Fang Tsay, Kriss Vissenberg for the seed lines. We thank NASC (Ohio State University) for providing T-DNA lines seed lines. J.M.E. is investigator of the National Research Council (CONICET) from Argentina. M.I. is supported by ANID FONDECYT POSTDOCTORADO [grant 3220138]. This work was supported by grants Natural Science Foundation of China (NSFC-32001974 and NSFC-31871396) to F.Y. and from ANPCyT (PICT2017-0066, and PICT2019-0015), by ANID – Programa Iniciativa Científica Milenio ICN17_022, NCN2021_010 and Fondo Nacional de Desarrollo Científico y Tecnológico [1200010] to J.M.E.

Author Contribution

J.M.P performed most of the experiments, analysed the data and helped in the writing process of the manuscript. L.S. performed the S6K-p determinations, IP of TOR-FER and immunolocalization assay of TOR. V.B.G., J.M.P., T.U.I., M.A.I., S-Z., Y.S., helped in the data analysis and writing process of the manuscript. F.Y. designed research and analysed part of the data and J.M.E. designed research, analysed the data, supervised the project, and wrote the paper. All authors commented on the results and the manuscript. This manuscript has not been published and is not under consideration for publication elsewhere. All the authors have read the manuscript and have approved this submission.

Competing financial interest

The authors declare no competing financial interests. Correspondence and requests for materials should be addressed to F.Y. (feng_yu@hnu.edu.cn) and J.M.E. (Email: jestevez@leloir.org.ar).

REFERENCES

1. Vijayakumar, P., Datta, S. & Dolan, L. ROOT HAIR DEFECTIVE SIX-LIKE4 (RSL4) promotes root hair elongation by transcriptionally regulating the expression of genes required for cell growth. *New Phytol.* **212**, 944–953 (2016).
2. Zhu, S. *et al.* The RALF1–FERONIA Complex Phosphorylates eIF4E1 to Promote Protein Synthesis and Polar Root Hair Growth. *Mol. Plant* (2020) doi:10.1016/j.molp.2019.12.014.
3. Yi, K., Menand, B., Bell, E. & Dolan, L. A basic helix-loop-helix transcription factor controls cell growth and size in root hairs. *Nat. Genet.* **42**, 264–267 (2010).
4. Datta, S., Prescott, H. & Dolan, L. Intensity of a pulse of RSL4 transcription factor synthesis determines Arabidopsis root hair cell size. *Nat. Plants* **1**, 1–6 (2015).
5. Vatter, T., Neuhäuser, B., Stetter, M. & Ludewig, U. Regulation of length and density of Arabidopsis root hairs by ammonium and nitrate. *J. Plant Res.* **128**, 839–848 (2015).
6. Canales, J., Contreras-López, O., Álvarez, J. M. & Gutiérrez, R. A. Nitrate induction of root hair density is mediated by TGA1/TGA4 and CPC transcription factors in Arabidopsis thaliana. *Plant J.* **92**, 305–316 (2017).
7. Liu, B., Wu, J., Yang, S., Schiefelbein, J. & Gan, Y. Nitrate regulation of lateral root and root hair development in plants. *Journal of Experimental Botany* vol. 71 4405–4414 (2020).
8. Ho, C. H., Lin, S. H., Hu, H. C. & Tsay, Y. F. CHL1 Functions as a Nitrate Sensor in Plants. *Cell* **138**, 1184–1194 (2009).
9. Gojon, A., Krouk, G., Perrine-Walker, F. & Laugier, E. Nitrate transceptor(s) in plants. *J. Exp. Bot.* **62**, 2299–2308 (2011).
10. Bouguyon, E. *et al.* Multiple mechanisms of nitrate sensing by Arabidopsis nitrate transceptor NRT1.1. *Nat. Plants* **1**, 15015 (2015).
11. Krouk, G. *et al.* Nitrate-regulated auxin transport by NRT1.1 defines a mechanism for nutrient sensing in plants. *Dev. Cell* **18**, 927–937 (2010).
12. Liu, K.-H. & Tsay, Y.-F. Switching between the two action modes of the dual-affinity nitrate transporter CHL1 by phosphorylation. *EMBO J.* **22**, 1005–13 (2003).
13. Forde, B. G. & Walch-Liu, P. Nitrate and glutamate as environmental cues for behavioural responses in plant roots. *Plant, Cell Environ.* **32**, 682–693 (2009).
14. Léran, S. *et al.* A unified nomenclature of nitrate transporter 1/peptide transporter family members in plants. *Trends in Plant Science* vol. 19 5–9 (2014).
15. Wang, W., Hu, B., Li, A. & Chu, C. NRT1.1s in plants: Functions beyond nitrate transport. *J. Exp. Bot.* **71**, 4373–4379 (2020).
16. Moison, M. *et al.* The lncRNA APOLO interacts with the transcription factor WRKY42 to trigger root hair cell expansion in response to cold. *Mol. Plant* **14**, 937–948 (2021).
17. Xiong, Y. & Sheen, J. The role of target of rapamycin signaling networks in plant growth and metabolism. *Plant Physiol.* **164**, 499–512 (2014).
18. Dobrenel, T. *et al.* The arabidopsis TOR kinase specifically regulates the expression of nuclear genes coding for plastidic ribosomal proteins and the phosphorylation of the cytosolic ribosomal protein S6. *Front. Plant Sci.* **7**, 1–16 (2016).
19. Saxton, R. A. & Sabatini, D. M. mTOR Signaling in Growth, Metabolism, and Disease. *Cell* **168**, 960–976 (2017).
20. Tatebe, H. & Shiozaki, K. Evolutionary Conservation of the Components in the TOR

549 Signaling Pathways. *Biomolecules* **7**, 1–17 (2017).
550 21. Van Leene, J. *et al.* Capturing the phosphorylation and protein interaction landscape of the
551 plant TOR kinase. *Nat. Plants* **5**, 316–327 (2019).
552 22. Menand, B. *et al.* Expression and disruption of the Arabidopsis TOR (target of rapamycin)
553 gene. *Proc. Natl. Acad. Sci. U. S. A.* **99**, 6422–6427 (2002).
554 23. Anderson, G. H., Veit, B. & Hanson, M. R. The Arabidopsis AtRaptor genes are essential for
555 post-embryonic plant growth. *BMC Biol.* **3**, 1–12 (2005).
556 24. Deprost, D., Truong, H. N., Robaglia, C. & Meyer, C. An Arabidopsis homolog of
557 RAPTOR/KOG1 is essential for early embryo development. *Biochem. Biophys. Res.*
558 *Commun.* **326**, 844–850 (2005).
559 25. Mahfouz, M. M., Kim, S., Delauney, A. J. & Verma, D. P. S. Arabidopsis TARGET of
560 RAPAMYCIN interacts with RAPTOR, which regulates the activity of S6 kinase in response to
561 osmotic stress signals. *Plant Cell* **18**, 477–490 (2006).
562 26. Yang, H. *et al.* MTOR kinase structure, mechanism and regulation. *Nature* **497**, 217–223
563 (2013).
564 27. Rexin, D., Meyer, C., Robaglia, C. & Veit, B. TOR signalling in plants. *Biochem. J.* **470**, 1–14
565 (2015).
566 28. Salem, M. A., Li, Y., Wiszniewski, A. & Giavalisco, P. Regulatory-associated protein of TOR
567 (RAPTOR) alters the hormonal and metabolic composition of Arabidopsis seeds, controlling
568 seed morphology, viability and germination potential. *Plant J.* **92**, 525–545 (2017).
569 29. Moreau, M. *et al.* Mutations in the Arabidopsis homolog of LST8/GβL, a partner of the
570 target of Rapamycin kinase, impair plant growth, flowering, and metabolic adaptation to
571 long days. *Plant Cell* **24**, 463–481 (2012).
572 30. McCready, K., Spencer, V. & Kim, M. The Importance of TOR Kinase in Plant Development.
573 *Front. Plant Sci.* **11**, 1–7 (2020).
574 31. Henriques, R. *et al.* Arabidopsis S6 kinase mutants display chromosome instability and
575 altered RBR1-E2F pathway activity. *EMBO J.* **29**, 2979–2993 (2010).
576 32. Ahn, C. S., Han, J. A., Lee, H. S., Lee, S. & Pai, H. S. The PP2A regulatory subunit Tap46, a
577 component of the TOR signaling pathway, modulates growth and metabolism in plants.
578 *Plant Cell* **23**, 185–209 (2011).
579 33. Xiong, Y. & Sheen, J. Rapamycin and glucose-target of rapamycin (TOR) protein signaling in
580 plants. *J. Biol. Chem.* **287**, 2836–2842 (2012).
581 34. Patrick, R. M. *et al.* Discovery and characterization of conserved binding of eIF4E 1 (CBE1),
582 a eukaryotic translation initiation factor 4E– binding plant protein. *J. Biol. Chem.* **293**,
583 17240–17247 (2018).
584 35. Xiong, Y. & Sheen, J. Novel links in the plant TOR kinase signaling network. *Curr. Opin. Plant*
585 *Biol.* **28**, 83–91 (2015).
586 36. Dobrenel, T. *et al.* TOR Signaling and Nutrient Sensing. *Annu. Rev. Plant Biol.* **67**, 261–285
587 (2016).
588 37. González, A. & Hall, M. N. Nutrient sensing and TOR signaling in yeast and mammals .
589 *EMBO J.* **36**, 397–408 (2017).
590 38. Bakshi, A., Moin, M., Madhav, M. S. & Kirti, P. B. Target of rapamycin, a master regulator of
591 multiple signalling pathways and a potential candidate gene for crop improvement. *Plant*

Biology vol. 21 190–205 (2019).

39. Pacheco, J. M. *et al.* The tip of the iceberg: emerging roles of TORC1, and its regulatory functions in plant cells. *J. Exp. Bot.* **72**, 4085–4101 (2021).
40. Dong, Y. *et al.* Sulfur availability regulates plant growth via glucose-TOR signaling. *Nat. Commun.* **8**, 1–10 (2017).
41. Cao, P. *et al.* Homeostasis of branched-chain amino acids is critical for the activity of TOR signaling in Arabidopsis. *Elife* **8**, 1–24 (2019).
42. Schaufelberger, M. *et al.* Mutations in the Arabidopsis ROL17/isopropylmalate synthase 1 locus alter amino acid content, modify the TOR network, and suppress the root hair cell development mutant lrx1. *J. Exp. Bot.* **70**, 2313–2323 (2019).
43. Sun, X. *et al.* Low nitrogen induces root elongation via auxin-induced acid growth and auxin-regulated target of rapamycin (TOR) pathway in maize. *J. Plant Physiol.* **254**, 153281 (2020).
44. Liu, Y. *et al.* Diverse nitrogen signals activate convergent ROP2-TOR signaling in Arabidopsis. *Dev. Cell* **56**, 1283-1295.e5 (2021).
45. Schepetilnikov, M. *et al.* GTP ase ROP 2 binds and promotes activation of target of rapamycin, TOR , in response to auxin . *EMBO J.* **36**, 886–903 (2017).
46. Li, X. *et al.* Differential TOR activation and cell proliferation in Arabidopsis root and shoot apexes. *Proc. Natl. Acad. Sci. U. S. A.* **114**, 2765–2770 (2017).
47. Carol, R. J. *et al.* A RhoGDP dissociation inhibitor spatially regulates growth in root hair cells. *Nature* **438**, 1013–1016 (2005).
48. Duan, Q., Kita, D., Li, C., Cheung, A. Y. & Wu, H. M. FERONIA receptor-like kinase regulates RHO GTPase signaling of root hair development. *Proc. Natl. Acad. Sci. U. S. A.* **107**, 17821–17826 (2010).
49. Kang, E. *et al.* The microtubule-associated protein MAP18 affects ROP2 GTPase activity during root hair growth. *Plant Physiol.* **174**, 202–222 (2017).
50. Denninger, P. *et al.* Distinct RopGEFs Successively Drive Polarization and Outgrowth of Root Hairs. *Curr. Biol.* **29**, 1854-1865.e5 (2019).
51. Huang, G. Q. *et al.* Arabidopsis RopGEF4 and RopGEF10 are important for FERONIA-mediated developmental but not environmental regulation of root hair growth. *New Phytol.* **200**, 1089–1101 (2013).
52. Xu, G. *et al.* FERONIA phosphorylates E3 ubiquitin ligase ATL6 to modulate the stability of 14-3-3 proteins in response to the carbon/nitrogen ratio. *J. Exp. Bot.* **70**, 6375–6388 (2019).
53. Pacheco, J. M. *et al.* The lncRNA APOLO and the transcription factor WRKY42 target common cell wall EXTENSIN encoding genes to trigger root hair cell elongation. *Plant Signal. Behav.* **16**, 1920191 (2021).
54. Kwon, T., Alan Sparks, J., Liao, F. & Blancaflor, E. B. Erulus is a plasma membrane-localized receptor-like kinase that specifies root hair growth by maintaining tip-focused cytoplasmic calcium oscillations[OPEN]. *Plant Cell* vol. 30 1173–1177 (2018).
55. Schoenaers, S. *et al.* The Auxin-Regulated CrRLK1L Kinase ERULUS Controls Cell Wall Composition during Root Hair Tip Growth. *Curr. Biol.* **28**, 722-732.e6 (2018).
56. Xiong, Y. *et al.* Glucose-TOR signalling reprograms the transcriptome and activates

meristems. *Nature* **496**, 181–186 (2013).
57. Montané, M. H. & Menand, B. ATP-competitive mTOR kinase inhibitors delay plant growth by triggering early differentiation of meristematic cells but no developmental patterning change. *J. Exp. Bot.* **64**, 4361–4374 (2013).
58. Escobar-Restrepo, J. M. *et al.* The Feronia receptor-like kinase mediates male-female interactions during pollen tube reception. *Science (80-.).* **317**, 656–660 (2007).
59. Haruta, M., Sabat, G., Stecker, K., Minkoff, B. B. & Sussman, M. R. A peptide hormone and its receptor protein kinase regulate plant cell expansion. *Science (80-.).* **343**, 408–411 (2014).
60. Chakravorty, D., Yu, Y. & Assmann, S. M. A kinase-dead version of FERONIA receptor-like kinase has dose-dependent impacts on rosette morphology and RALF1-mediated stomatal movements. *FEBS Lett.* **592**, 3429–3437 (2018).
61. Deprost, D. *et al.* The Arabidopsis TOR kinase links plant growth, yield, stress resistance and mRNA translation. *EMBO Rep.* **8**, 864–870 (2007).
62. Jones, M. A. *et al.* The arabidopsis Rop2 GTPase is a positive regulator of both root hair initiation and tip growth. *Plant Cell* **14**, 763–776 (2002).
63. Gendre, D. *et al.* Rho-of-plant activated root hair formation requires arabidopsis YIP4a/b gene function. *Dev.* **146**, (2019).
64. Zhu, S., Martínez Pacheco, J., Estevez, J. M. & Yu, F. Autocrine regulation of root hair size by the RALF-FERONIA-RSL4 signaling pathway. *New Phytol.* **227**, 45–49 (2020).
65. Song, Y. *et al.* FERONIA restricts Pseudomonas in the rhizosphere microbiome via regulation of reactive oxygen species. *Nat. Plants* **7**, 644–654 (2021).
66. Livak, K. J. & Schmittgen, T. D. Analysis of relative gene expression data using real-time quantitative PCR and the 2-ΔΔCT method. *Methods* **25**, 402–408 (2001).